J. Membrane Biol. 164, 11–24 (1998)

The Journal of
Membrane
Biology

Transmembrane Mg^{2+} Currents and Intracellular Free Mg^{2+} Concentration in *Paramecium tetraurelia*

R.R. Preston

Department of Physiology, Allegheny University of the Health Sciences, Philadelphia, PA 19129, USA

Received: 12 January 1998/Revised: 16 March 1998

Abstract. The properties of Mg^{2+} conductances in *Paramecium tetraurelia* were investigated under two-electrode voltage clamp. When bathed in physiological Mg^{2+} concentrations (0.5 mM), depolarizing steps from rest elicited a prominent Mg^{2+}-specific current (I_{Mg}) that has been noted previously. The dependence of this current on extracellular Mg^{2+} approximated that of Mg^{2+}-induced backward swimming, demonstrating that I_{Mg} contributes to normal membrane excitation and behavior in this ciliate. Closer analysis revealed that the Mg^{2+} current deactivated biphasically. While this might suggest the involvement of two Mg^{2+}-specific pathways, both tail-current components were affected similarly by current-specific mutations and they had similar ion selectivities, suggesting a common pathway. In contrast, a Mg^{2+} current activated upon hyperpolarization could be separated into three components. The first, I_{Mg}, had similar properties to the current activated upon depolarization. The second was a nonspecific divalent cation current (I_{NS}) that was revealed following suppression of I_{Mg} by *eccentric* mutation. The final current was relatively minor and was revealed following suppression of I_{Mg} and I_{NS} by *obstinate A* gene mutation. Reversal-potential analyses suggested that I_{Mg} and I_{NS} define two intracellular compartments that contain, respectively, low (0.4 mM) and high (8 mM) concentrations of Mg^{2+}. Measurement of intracellular free Mg^{2+} using the fluorescent dye, Mag-fura-2, suggested that bulk $[Mg^{2+}]_i$ rests at around 0.4 mM in *Paramecium.*

Key words: *Paramecium* — Mg^{2+} behavior — Mg^{2+} current — Mutation — Intracellular free Mg^{2+} homeostasis — Mag-fura-2

Correspondence to: R.R. Preston

Introduction

Recent years have witnessed increasing support for the idea that intracellular free Mg^{2+} ($[Mg^{2+}]_i$) may be a critical regulator of cell activity in eukaryotes (Grubbs & Maguire, 1987; White & Hartzell, 1989; Romani & Scarpa, 1992). This notion has been fueled by finding that most cells maintain $[Mg^{2+}]_i$ in the range of 0.2 to 0.8 mM (Alvarez-Leefmans, Giraldez & Gamiño, 1987). Although extracellular free Mg^{2+} is typically not much greater than $[Mg^{2+}]_i$ (plasma contains about 0.8 mM), a cell's negative membrane potential provides a strong driving force for Mg^{2+} influx. Indeed, if Mg^{2+} were in equilibrium across the plasma membrane, internal values should be of the order of 5 to 200 mM. Maintaining a low $[Mg^{2+}]_i$ thus requires that cells continually remove this cation from the cytoplasm, and this is accomplished using Mg^{2+}-specific transporters (reviewed by Beyenbach, 1990; Flatman, 1991). Most eukaryotic cells appear to contain a Na^+/Mg^{2+} exchanger that uses the transmembrane Na^+ gradient to expel Mg^{2+} (Beyenbach, 1990; Günther & Ebel, 1990; Flatman, 1991) and there is also evidence for Mg^{2+}:Cl^- and Mg^{2+}:H^+ cotransporters (Günther & Vormann, 1990; Amalou et al., 1994). While these observations are interesting in their own right, their true significance becomes apparent only when one considers that many of the enzymes involved in basic cellular functions are Mg^{2+}-dependent and/or Mg^{2+}-regulated (Cowan, 1995). Further, their requirement for Mg^{2+} often approximates $[Mg^{2+}]_i$, suggesting that even small changes in internal levels could have dramatic effects on cell activity. There are now many reports of extracellular factors causing changes in $[Mg^{2+}]_i$ (Paolisso et al., 1986; Grubbs & Maguire, 1987; Gylfe, 1990; Grubbs, 1991; Ishijima, Sonoda & Tatibana, 1991; Dai & Quamme, 1992; Okada, Ishikawa & Saito, 1992; Hwang, Yen & Nadler, 1993; Singh & Wisdom, 1995; Sébille et al., 1996) but, while these results are tantaliz-

ing, showing that hormone-induced changes in $[Mg^{2+}]_i$ couple reception of a stimulus with a specific cellular response has proved difficult. This is due in part to the fact that when changes in $[Mg^{2+}]_i$ have been observed, they are often relatively small and occur over several minutes. This makes it difficult to determine their possible functions.

Attempts to better understand how changes in $[Mg^{2+}]_i$ affect eukaryotic cells have included studies of a Mg^{2+}-specific conductance in *Paramecium* (Preston, 1990). Though a protozoan, *Paramecium* possesses a sophisticated excitable membrane that bears many characteristics common to neurons and secretory cells (Hinrichsen & Schultz, 1988). Excitation in *Paramecium* involves Ca^{2+} influx through voltage-sensitive channels in the ciliary membrane. Ca^{2+} then acts as a second messenger to cause ciliary reversal and backward swimming away from the stimulus (reviewed by Preston & Saimi, 1990). Ca^{2+} influx also elicits a Mg^{2+}-specific current, I_{Mg}. While Mg^{2+} fluxes have been described in other excitable cells, they usually occur *via* Ca^{2+} channels or nonspecific cation channels (Nakatani & Yau, 1988; Narita, Kawasaki & Kita, 1990; Kawa, 1996). I_{Mg} in *Paramecium* is unusual because Mg^{2+} is the preferred change carrier and because Ca^{2+} is impermeant, a selectivity sequence sets it apart from most other known ion channels. Perhaps most interestingly, I_{Mg} activates rapidly upon membrane excitation and the resultant Mg^{2+} flux is sufficiently large that it could change $[Mg^{2+}]_i$ significantly. The rapid kinetics and magnitude of this current means that it is easy to study and manipulate using conventional electrophysiological techniques. Furthermore, mutations are available that either specifically suppress (''*eccentric A*'', Preston & Kung, 1994*a*,*b*) or potentiate (''*chameleon*'', Preston & Hammond, 1997) this current. *Eccentric* provides a living control that allows the experimenter to distinguish changes caused by Mg^{2+} influx from those associated with Mg^{2+} acting extracellularly, whereas *chameleon* provides a way of enhancing and highlighting intracellular effects. Thus, I_{Mg} in *Paramecium* presents a unique and invaluable opportunity to determine the consequences of physiological changes in $[Mg^{2+}]_i$ in a eukaryotic cell.

Initial characterization of I_{Mg} in *Paramecium* was brief and was performed using much higher concentrations of Mg^{2+} extracellularly than are found in freshwater (5 mM, *c.f.* the 0.2 to 0.7 mM Mg^{2+} found in soft and hard water, respectively, Machemer & Deitmer, 1985). This has raised questions about the physiological significance of I_{Mg} in vivo. The present study investigates I_{Mg} in more detail and at physiological Mg^{2+} concentrations. It takes advantage of the availability of the I_{Mg}-deficient *eccentric* mutant and of a newly isolated mutant that lacks I_{Mg} upon hyperpolarization (''*obstinate A*'') to reveal a Mg^{2+}-permeable but nonspecific cation conductance in *Paramecium.* Finally, evidence is presented that suggests that Mg^{2+} may be compartmentalized within *Paramecium.*

Materials and Methods

Cell Stocks and Culture Conditions

The present studies were conducted using a wild-type stock of *Paramecium tetraurelia* (stock 51, sensitive) and three mutants derived from this stock: d4-95 *pawn B* (Kung, 1971*a*,*b*), d4-700 *eccentric A* (Preston & Kung, 1994*b*) and pa-716 *obstinate A* (*unpublished*). All stocks also contained *nd6*, a trichocyst non-discharge mutation (Lefort-Tran et al., 1981). Cells were raised at 23°C on ''C7'', a semi-defined culture medium similar to that used previously (Preston, Saimi & Kung, 1990). This medium contained 0.2 mM $MgSO_4$, 0.5 mM $CaCl_2$, 0.5 mM K_2HPO_4, 0.1 g/l NH_4-acetate, 0.2 g/l glucose, 3 mM NaOH, 0.5 mg/l stigmasterol, 7.5 mg/l phenol red, 5 mM HEPES buffer and was inoculated with *Enterobacter aerogenes* prior to introducing paramecia.

Solutions

Unless stated otherwise, all solutions contained (in mM): 1 Ca^{2+} (0.25 $Ca(OH)_2$ + 0.75 $CaCl_2$), 0.01 EDTA, 1 HEPES buffer, pH 7.2. Chloride salts of other ions were added as required. 'Resting solution' additionally contained 4 mM KCl. ''Dye buffer'' contained (in mM) 5 Na^+, 2 Mg^{2+} and 1 K^+. Studies of the Mg^{2+} current (including investigations into its specificity) used solutions supplemented with 10 tetraethylammonium (TEA) Cl to block K^+ currents.

Behavioral Testing

A sample of cells (15–20 individuals) was transferred from growth medium to resting solution where they remained for 10 min. Individuals were then selected using a micropipette under low-power magnification and ejected into a solution containing Mg^{2+}. The duration of evoked backward swimming was timed using a stopwatch.

Intracellular Recording

Membrane currents were recorded using established voltage-clamp techniques (Hinrichsen & Saimi, 1984; Preston, Saimi & Kung, 1992). The two intracellular capillary microelectrodes used for clamping the membrane contained either 3 M KCl (when recording K^+ currents) or 4 M CsCl (when recording Mg^{2+} currents), tip resistance 10–25 MΩ. Currents were filtered at 1–2 kHz. All experiments were performed at room temperature (22.5–25°C).

Data Analysis

Data were collected and analyzed using pCLAMP software (Axon Instruments, Foster City, CA). All currents were leak-corrected on the basis of linear responses induced by −3 to −12 mV steps of 20-msec duration. Membrane capacitance was determined from the time course of membrane voltage responses to 0.2 nA current injections (100 msec). Capacitive transients elicited by step changes in membrane potential required up to 0.6 msec to settle, so tail current analyses excluded the initial 1–2 msec of the trace. Current amplitudes at the instant of stepping to a new voltage level were then determined by

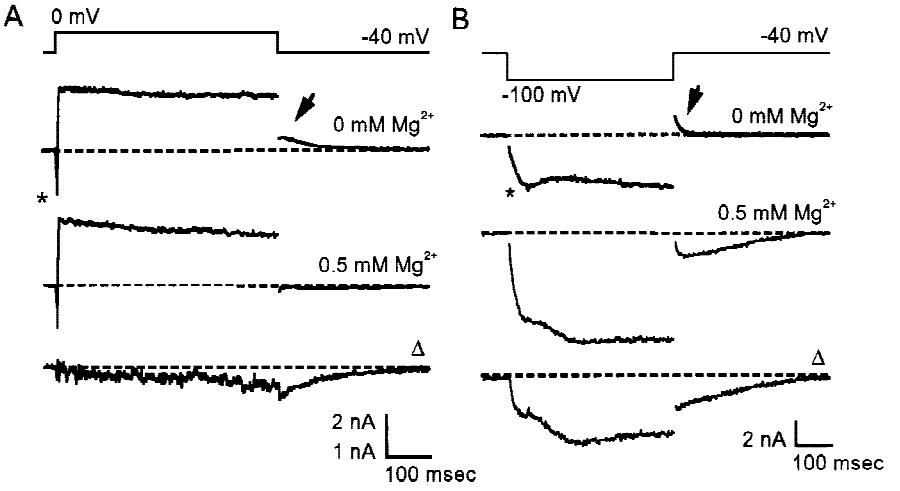

Fig. 1. Currents activated in the presence of extracellular Mg^{2+}. (*A*) Currents upon depolarization. Currents were activated by 500-msec steps from −40 to 0 mV under voltage clamp (membrane potential trace: *top*). *Upper current trace* shows membrane response in a Mg^{2+}-free solution containing 1 mM K^+ and 1 mM Ca^{2+} (*see* Materials and Methods). The initial inward transient (*asterisk*) reflected activation of $I_{Ca(d)}$, followed by two outward K^+ currents. The *arrow* indicates the slow decay of the tail current associated with $I_{K(Ca,d)}$. *Middle current trace* was elicited after adding 0.5 mM Mg^{2+} to the bath solution. Digital subtraction of the previous trace from the response in Mg^{2+} yielded a difference current that approximated I_{Mg} (*lower current trace*). Note that the *lower trace* has been scaled by a factor of two to better show development of the inward current. (*B*) Current elicited by 500-msec step hyperpolarizations from −40 to −100 mV (voltage trace, *top*). In the absence of Mg^{2+}, the voltage step elicited an inward Ca^{2+} transient ($I_{Ca(h)}$; *asterisk*) and two inward K^+ currents (*upper current trace*). The arrow indicates the decay of $I_{K(h)}$ and $I_{K(Ca,h)}$ tail currents. Adding 0.5 mM Mg^{2+} to the bath potentiated the inward current and promoted a slow inward tail current upon returning to −40 mV (*middle current trace*). The difference current (*lower current trace*) is a rough approximation of I_{Mg} upon hyperpolarization. Traces in this and all subsequent figures have been corrected for linear leak current (*see* Materials and Methods). Broken lines represent holding current.

back-extrapolation. When determining the Mg^{2+}-concentration dependence of currents, cells were stepped for 500 msec from holding potential (between −40 and −30 mV depending on $[Mg^{2+}]_o$) to potentials that were 20 mV beyond that required to elicit a maximal (for currents activated upon depolarization) or saturating (for currents activated upon hyperpolarization) inward tail current (a voltage excursion of ≤140 mV). All data are presented as means ±SD, and were compared statistically using a Student's *t*-test: *P* values < 0.05 were considered significant.

Spectrophotometric Determination of $[Mg^{2+}]_i$

$[Mg^{2+}]_i$ was estimated using the fluorescent probe, mag-fura-2 (Molecular Probes, OR). A 500-ml sample of cells in logarithmic growth was concentrated by centrifugation then washed and resuspended in 2.5 ml of dye buffer. Membrane-permeant dye (mag-fura-2 AM) was added (20 μg dissolved in 20 μl anhydrous DMSO) and loading conducted in the dark at 28°C for 1 hr. Cells were then washed into 100 ml of fresh dye buffer and incubated in the dark at room temperature for 1 hr to allow for dye conversion. The cells were then concentrated and transferred in 1.8 ml of dye buffer to a stirred quartz cuvette placed within the excitation beam of a SLM-Aminico 4000 spectrofluorometer. $[Mg^{2+}]_i$ was calculated using the following equation (*see* Grynkiewicz, Poenie & Tsien, 1985):

$$[Mg^{2+}] = K_d Q \frac{(R - R_{min})}{(R_{max} - R)}$$

where R is the ratio of mag-fura-2 fluorescence intensity recorded at 490 nm using excitation wavelengths of 320 nm (for Mg^{2+}-complexed dye) and 390 nm (Mg^{2+}-free dye), R_{min} is the ratio in the absence of $[Mg^{2+}]_o$ (chelated using 3 mM EDTA) and R_{max} is the ratio in the presence of 12 mM $[Mg^{2+}]_o$. R_{min} and R_{max} were determined after permeabilizing the cells with 0.02% Triton X-100. Q was determined from the ratio of emissions from Mg^{2+}-free and Mg^{2+}-complexed dye using an excitation wavelength of 390 nm. K_d of mag-fura for Mg^{2+} *in vivo* has been calculated to be 1.5 mM (Raju et al., 1989; Grubbs & Walter, 1994).

Results

Activating I_{Mg} Under Physiological Conditions

Early studies of *Paramecium* behavior and electrophysiology routinely used simple experimental solutions containing 1–4 mM K^+, 1 mM Ca^{2+} and 1 mM Tris, MOPS or HEPES buffer. These solutions were designed to mimic freshwater, *Paramecium's* natural habitat. Depolarizing *Paramecium* in such a solution (''resting solution'') elicited an inward Ca^{2+} current ($I_{Ca(d)}$; Fig. 1*A*, *upper current trace*, *asterisk*) followed by two outward K^+ currents. Returning to −40 from 0 mV evoked a slow ($\tau \cong$ 100 msec) outward tail current caused by K^+-current deactivation (Fig. 1*A*, *arrow*). The Ca^{2+} current normally provides the rise in $[Ca^{2+}]_i$ that drives ciliary reversal and backward swimming in *Paramecium*, whereas the K^+ currents help repolarize the membrane and restore forward swimming. All three currents have been described

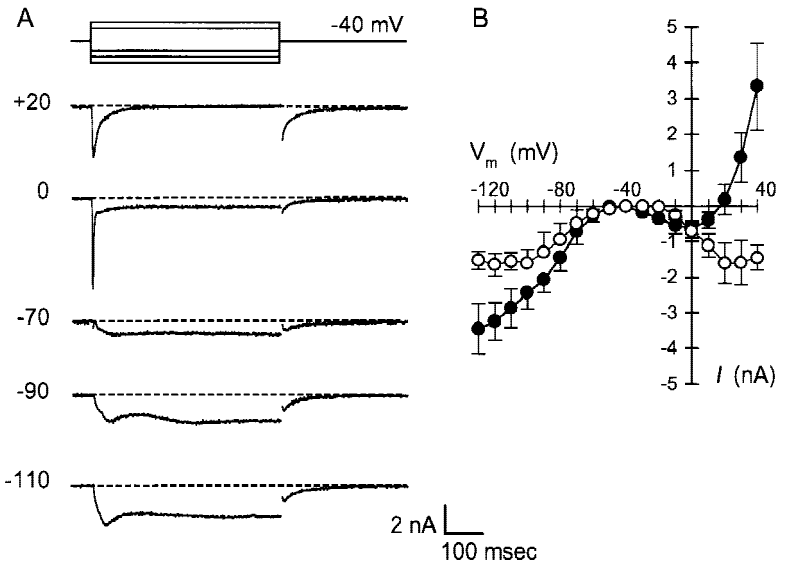

Fig. 2. I_{Mg} in *Paramecium.* (*A*) Currents were elicited in 0.5 mM Mg^{2+} and 1 mM Ca^{2+} (after suppressing K^+ currents with Cs^+ and TEA^+: *see* Materials and Methods) using 500-msec steps to 20, 0, −70, −90 or −110 mV (voltage trace, *top*). (*B*) Amplitudes of the currents measured at 500 msec immediately before returning to −40 mV (*filled circles*) and of resultant tail currents (*open circles*) are plotted as a function of membrane potential at which they were elicited (V_m). Points represent means ± SD from 13 cells. Currents (*I*) have been leak-corrected.

previously (Oertel, Schein & Kung, 1977; Saimi et al., 1983). Hyperpolarizing *Paramecium* under these same conditions elicited a similar yet distinct set of currents. The peak inward current in Fig. 1*B* (*upper trace, asterisk*) comprised a novel hyperpolarization-activated Ca^{2+} current ($I_{Ca(h)}$) and a K^+ current. Both currents inactivated during the voltage step, but Ca^{2+} entering the cell via $I_{Ca(h)}$ then activated a Ca^{2+}-dependent K^+ current that developed slowly during the step and was sustained for at least 2 sec (Preston et al., 1990). The outward tail current upon returning to rest (Fig. 1*B, upper trace, arrow*) reflected K^+-current deactivation. These three currents have also been described previously (Oertel, Schein & Kung, 1978; Preston et al., 1990, 1992; Richard, Saimi & Kung, 1986).

Freshwater contains Mg^{2+} in addition to K^+ and Ca^{2+}. The concentration varies according to the degree of hardness, but is typically around 0.2–0.7 mM (*see* Machemer & Deitmer, 1985). When a physiological concentration of Mg^{2+} (0.5 mM) was added to resting solution, the outward current elicited by step depolarization was reduced slightly and the tail now comprised both outward and inward components (Fig. 1*A, middle trace*). Step hyperpolarization in the presence of Mg^{2+} yielded an inward current that was increased compared with the response in Mg^{2+}-free resting solution, while returning to −40 mV elicited a prominent, slow, inward tail (Fig. 1*B, middle trace*). Subtracting the currents elicited in the absence of Mg^{2+} from those with 0.5 mM Mg^{2+} yielded difference currents (Fig. 1*A* and *B, lower traces*) that approximated a Mg^{2+}-specific conductance, I_{Mg} (Preston, 1990).

To examine I_{Mg} in isolation from the K^+ currents, the clamp microelectrodes were now filled with CsCl instead of KCl, while TEA^+ (10 mM) replaced K^+ in the bath. Cs^+ blocks K^+ currents intracellularly while TEA^+ blocks the K^+ currents extracellularly (Hinrichsen & Saimi, 1984; Preston et al., 1990) to yield Ca^{2+}- and Mg^{2+}-currents. TEA^+ had no significant effect on I_{Mg} (*not shown*). Step depolarization of *Paramecium* under these conditions again elicited $I_{Ca(d)}$ which activated rapidly and then inactivated within milliseconds (Fig. 2, *upper two traces*). Returning to −40 mV evoked a slow inward tail current representing deactivation of I_{Mg}. Step hyperpolarization also elicited an inactivating Ca^{2+} current ($I_{Ca(h)}$), followed at *ca.* 200 msec by the slower-activating Mg^{2+} current (Fig. 2*A, lower three traces*). Again, a return to −40 mV following step hyperpolarization was accompanied by a slow inward tail. The relationship between currents measured at the end of the 500-msec voltage step and membrane potential (V_m) was *N*-shaped (Fig. 2*B, filled circles*). This is because while hyperpolarization always activated inward currents, positive steps elicited inward currents at −30 to 10 mV and outward currents at ⩾20 mV. The relationship between tail-current amplitudes and step size was bell-shaped (Fig. 2*B, open circles*), reflecting the fact that I_{Mg} could be activated by positive or negative steps from rest. Note that tail amplitudes saturated when the activating step reached *ca.* −100 or 20 mV.

Dependence of I_{Mg} on $[Mg^{2+}]_o$

V_m rests at −30 to −40 mV in the low-salt buffer solutions used here, providing a strong driving force for Mg^{2+} influx when extracellular concentrations are 20 μM or greater ($[Mg^{2+}]_i$ rests at around 0.4 mM; Preston, 1990). Thus, activating I_{Mg} depolarizes the membrane of a free-swimming cell and thereby potentiates and sustains Ca^{2+} influx via the depolarization-activated $I_{Ca(d)}$ to cause prolonged ciliary reversal and backward swim-

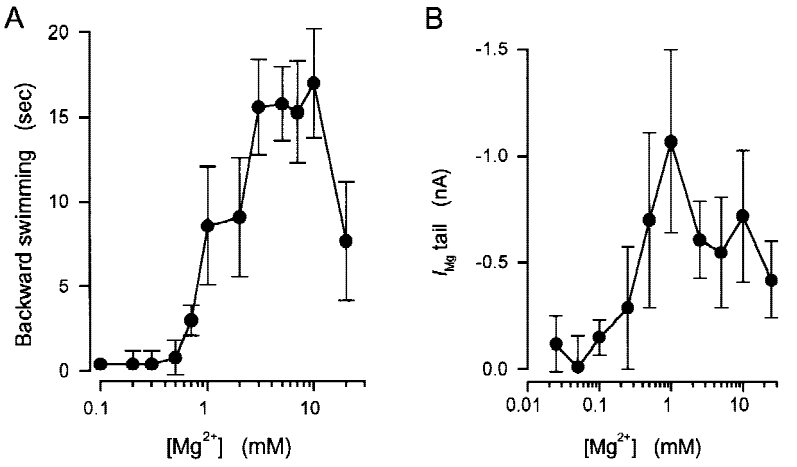

Fig. 3. Mg^{2+}-concentration dependence of behavioral excitation and of I_{Mg} activated upon depolarization. (*A*) Duration of backward swimming elicited upon transferring individual cells to solutions containing various concentrations of Mg^{2+}. Points are means ± SD from 10 cells. (*B*) Amplitudes of I_{Mg} tail currents elicited by 500-msec step depolarizations from cells under voltage clamp in various concentrations of Mg^{2+}. Points are means ± SD from 4–8 cells.

ming. The dependence of backward-swimming duration on $[Mg^{2+}]_o$ is shown in Fig. 3*A*. Mg^{2+} concentrations of <0.5 mM typically caused transient ciliary reversals and repeated turning (''Mg^{2+} dancing''). Concentrations of ⩾0.5 mM elicited sustained backward swimming, the duration of which increased with $[Mg^{2+}]_o$ to a peak at 3–10 mM and declined thereafter. To determine whether Mg^{2+}-induced backward swimming results from activation of I_{Mg}, the dependence of this current upon depolarization on extracellular Mg^{2+} concentration was examined also. Figure 3*B* shows that Mg^{2+} tail currents were first observed at >50 μM $[Mg^{2+}]_o$ and were maximal at 1 mM $[Mg^{2+}]_o$. Further increases in concentration yielded smaller currents (presumably due to Mg^{2+} inhibition of $I_{Ca(d)}$: *see* Discussion), much as increasing $[Mg^{2+}]_o$ above 10 mM reduced backward swimming durations compared with lower concentrations (Fig. 3*A*).

The concentration-dependence of the tail currents activated upon hyperpolarization is shown in Fig. 4. Whereas depolarization elicited Mg^{2+} tails that were always inward, the currents upon hyperpolarization were complex. The tails typically decayed with a time course that was best described using two exponential functions with time constants of around 10 msec and 150–250 msec (*see below*). However, whereas the slower-decaying component was inward at all Mg^{2+} concentrations tested, the faster-decaying component was outward at 25 μM–0.5 mM Mg^{2+} but then reversed polarity and was inward at ⩾1 mM (Fig. 4*B*). At 25 mM Mg^{2+} the two components were of approximately equal magnitude, their sum representing a current density of 24 pA/pF (±23 pA/pF, $n = 8$).

Development of I_{Mg} with Time

Previous studies always used 500-msec voltage steps to elicit I_{Mg}, so there is little sense as to how fast this current develops or for how long it remains active following excitation, although behavioral observations (Fig. 3*A*) suggested that it may persist for several seconds upon depolarization.

To examine this more directly, cells were held at −30 mV in 5 mM Mg^{2+} and then stepped to 20 mV for periods ranging from 10 msec to 2 sec. This produced a family of tail currents, as shown in Fig. 5*A*. The rationale behind this lay in the fact that whereas many independent conductances contribute to the current flowing during a voltage step, tail currents are relatively pure and may thus be used to investigate the kinetics of Mg^{2+} currents in isolation (Preston, 1990; Preston et al., 1990). The tail currents elicited by steps of short duration (10–50 msec) typically could be described by a single exponential function with a time constant of about 11 msec (Table). Step depolarizations of ⩾50 msec elicited tails that contained a second, slower exponential component with a time constant of *ca.* 150 msec (Table). The amplitudes of the two Mg^{2+} tail components have been plotted against the duration of the activating step in Fig. 5*B*, while their sum is shown in Fig. 5*C*. This suggested that I_{Mg} activated rapidly during depolarization toward a peak at 100–200 msec and then relaxed toward a new, sustained level at around 500 msec (Fig. 5*C*). I_{Mg} developed surprisingly fast during depolarization: a tail current with a time constant of 10.7 msec could be readily observed following a step depolarization of only 10 msec and by 30 msec was prominent (Fig. 6*A*, *arrow*). For comparison, Fig. 6*B* shows currents elicited by a similar voltage protocol from an *eccentric* mutant cell. *Eccentric* was isolated by virtue of its inability to respond to Mg^{2+} with backward swimming (Preston & Kung, 1994*b*) due to its loss of I_{Mg} (Preston & Kung, 1994*a; see* below).

The development of Mg^{2+} currents during step hyperpolarization (to −110 mV) of the wild type was investigated also (Fig. 7*A*). These tails also decayed biphasically and with similar time constants to the depo-

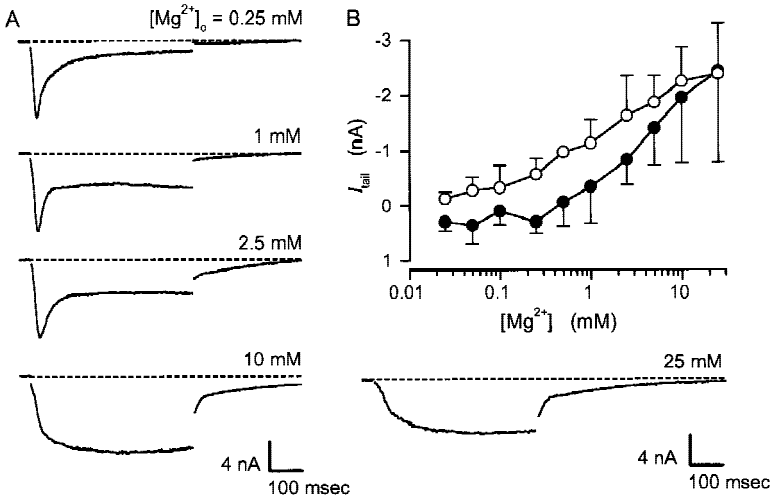

Fig. 4. Concentration-dependence of Mg^{2+} currents upon hyperpolarization. (*A*) Currents were elicited using 500-msec steps from −40 to −140 mV in 0.25 mM, 1 mM or 2.5 mM Mg^{2+}, or from −30 to −130 mV in 10 or 25 mM Mg^{2+}. (*B*) Amplitudes of the two tail-current components are plotted as a function of extracellular Mg^{2+} concentration. *Filled circles* indicate fast-decaying tail currents, whereas *open circles* indicate slow-decaying currents. Points are means ± SD from 3–8 cells.

larization-activated current. A fast-decaying tail component ($\tau \cong 15$ msec; Table) peaked rapidly at 50 msec and relaxed slowly over the subsequent 2 sec (Fig. 7*B, upper*). A slower-decaying component ($\tau \cong 160$ msec; Table) was apparent after steps of only 10-msec duration in some cells but became prominent at 50 msec and increased gradually toward a peak at 500 msec. This component then waned slowly over the subsequent 2 sec (Fig. 7*B*). The envelope of combined Mg^{2+} tails (Fig. 7*C*) resembled that of the depolarization-activated I_{Mg} (Fig. 5*C*); current developed rapidly toward a peak at *ca.* 50 msec, relaxed, rose toward a second peak at 200–300 msec and then subsided gradually.

Properties of the Mg^{2+} Current Elicited upon Depolarization

The finding that Mg^{2+} tails upon both depolarization and hyperpolarization could both be separated into fast- and slow-decaying components invited questions about the number of ion-channel species underlying these currents. To investigate these questions directly, *pawn B* mutant cells were depolarized for periods ranging from 25 msec to 2 sec (Fig. 8, *upper current trace*). *Pawns* lack the ciliary Ca^{2+} current (Oertel et al., 1977); the lack of an inward tail in the traces shown suggested that the two Mg^{2+} currents shared a common dependence on $I_{Ca(d)}$. *Eccentric A* specifically lacks I_{Mg}. It too was depolarized to 20 mV for periods ranging from 25 msec to 2 sec, but again there was no evidence of a Mg^{2+} tail (Fig. 8, *lower trace*).

Finally, the ion selectivity of the two tails was examined to see if they shared the strong preference for Mg^{2+} over Ca^{2+} that is the hallmark of I_{Mg} (Preston, 1990). Cells were held at −40 mV and then stepped for 500 msec to 20 mV in the presence of 1 mM Mg^{2+} or various other divalent cations (Fig. 9*A*). Magnitudes of

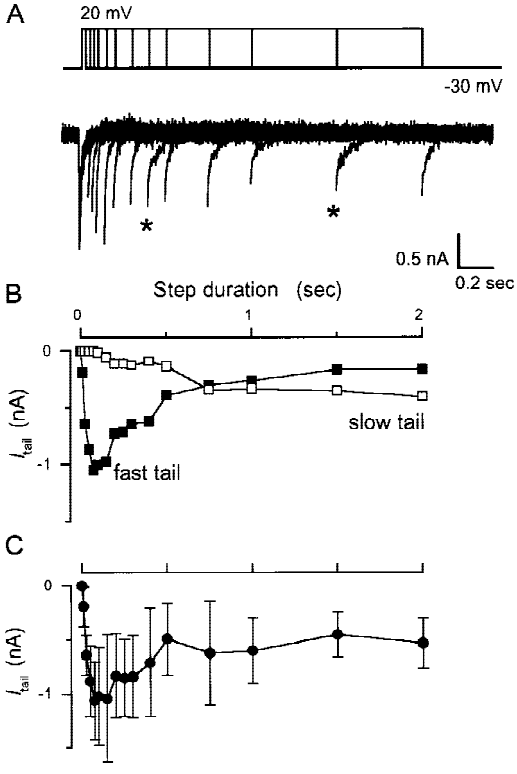

Fig. 5. Development of I_{Mg} upon depolarization. (*A*) Cells bathed in Mg^{2+} solution were held under voltage clamp at −30 mV and then stepped to 20 mV for periods ranging from 10 msec to 2 sec. Note that the amplitude of the tail currents can vary during collection of data from a single cell (*asterisks* indicate tails at 0.4 and 1.5 sec that are larger than might have been expected from the other tails in the sequence). This is normal and common and is believed to be related to the way in which $[Ca^{2+}]_i$ is regulated during depolarization, although this has not been investigated systematically. (*B*) Amplitudes of fast-decaying (*filled squares*) and slow-decaying (*open squares*) tail components plotted as a function of the duration of the step used to elicit current. (*C*) Combined amplitudes of fast and slow tails plotted as a function of step duration. Points are means ± SD from 16 cells.

Table. Summary of the properties of the tail currents elicited from wild-type and mutant cells in 5 mM Mg^{2+}

Cell stock	Activation step (mV)	Ion current	Tail kinetics	Time constant (msec)	Ion selectivity
Wild type	+20	I_{Mg}	Fast	11.2 ± 2.6(15)	$Mg^{2+} > Ba^{2+}$
	+20	I_{Mg}	Slow	148 ± 66 (15)	$Mg^{2+} > Ba^{2+}$
	−110	I_{NS}	Fast	14.6 ± 2.4(18)	$Mg^{2+} < Ba^{2+}$
	−110	I_{Mg}	Slow	156 ± 67 (18)	$Mg^{2+} > Ba^{2+}$
Eccentric	−110	I_{NS}	Fast	15.5 ± 2.9(11)	$Mg^{2+} < Ba^{2+}$
	−110	I_{Mg}, I_{obs}?	Slow	145 ± 95 (6)	*nd*
Obstinate	−110	I_{obs}	Intermediate	103 ± 42 (5)	*nd*

Tails were elicited using 50-msec or 1-sec steps from −30 mV to give currents with predominantly fast and slow kinetics, respectively. Data are means ± SD of (*n*) determinations. ''*nd*'' indicates that selectivity was not determined.

both tail components were greatest when Mg^{2+} was the charge carrier (Fig. 9*B*), but kinetically similar currents were observed when Mn^{2+} and Co^{2+} replaced Mg^{2+}. Substitution of Ba^{2+} or Ca^{2+} reduced significantly or suppressed the currents compared with those in Mg^{2+} (*see* Fig. 9, legend).

Properties of the Mg^{2+} Current Elicited upon Hyperpolarization

I_{Mg} activated upon hyperpolarization was subjected to a similar analysis. *Obstinate A* is a newly isolated mutant in which $I_{Ca(h)}$ is suppressed (*unpublished*). Steps to −110 mV of 10 msec to 2-sec duration elicited a minor inward tail current (<0.2 nA) with a time constant of about 100 msec (Table, Fig. 10), but there was no evidence of significant fast or slow tails comparable to those observed in the wild type (Fig. 7). Figure 11*A* shows currents elicited by step hyperpolarization of *eccentric*. Whereas depolarization had failed to elicit Mg^{2+} currents in this mutant (Fig. 8), hyperpolarizations of short duration (10–50 msec) produced fast-decaying tails (Table) that peaked at 50 msec and relaxed thereafter (Fig. 11*B*, *filled squares*). Steps of >50 msec often (in 6 of 11 cells examined) elicited a biexponential tail current. The second, slower component (Table) was slow to develop and relaxed slightly during the step (Fig. 11*B*, *open squares*).

Next, the ion selectivity of the fast and slow wild-type Mg^{2+} tails were compared. Currents were elicited using 500-msec steps to −110 mV in the presence of Mg^{2+} or various other divalent cations (Fig. 12*A*). Whereas the slow tail showed a similar selectivity to the tails upon depolarization ($Mg^{2+} > Ba^{2+}$, Ca^{2+}: Fig. 12*B*, *lower*), the fast-decaying tail surprisingly showed a preference for Ba^{2+}, Co^{2+}, and Mn^{2+} over Mg^{2+} (Fig. 12*B*, *upper*) although again there was no significant inward tail in Ca^{2+}. This implies that there may be two distinct Mg^{2+} conductances activated upon hyperpolarization of the wild type: I_{Mg} and a second divalent cation current that has a significant Ba^{2+} permeability (''I_{NS}''). This might explain how *eccentric* mutation could suppress I_{Mg} upon depolarization yet leave a residual current upon hyperpolarization. To explore this idea more fully, the selectivity of *eccentric's* Mg^{2+} tail was examined to determine whether its ionic preference matched that of I_{Mg} ($Mg^{2+} > Ba^{2+}$) or of the fast-decaying I_{NS} ($Mg^{2+} < Ba^{2+}$). The results are shown in Fig. 13. The slow tail component noted above appeared inconsistently and was too small to analyze in terms of its ion specificity. The fast component was considerably larger, however, and clearly showed a preference for Ba^{2+} and over Mg^{2+} (Fig. 13*B*).

Determination of $[Mg^{2+}]_i$ in the Wild Type and in *Eccentric*

The properties of the fast-decaying tail in *eccentric* were investigated further. Cells were hyperpolarized for 400 msec to elicit current and V_m was then stepped to potentials ranging from −70 to 20 mV (Fig. 14*A*, *top*). This elicited the Mg^{2+} currents described above and various other currents associated with membrane hyperpolarization and depolarization (Fig. 14*A*, *middle*). In order to subtract out the latter currents and analyze the behavior of the isolated Mg^{2+} tail, the voltage protocol in Fig. 14*A* was repeated after inactivating $I_{Ca(h)}$ and its dependent currents with 4.5-sec steps to −120 mV (Fig. 14*A* *lower*). Digital subtraction of the two sets of traces yielded difference currents (Fig. 14*B*) whose tails were clearly dependent on V_m (Fig. 14*C*). The current shown had a reversal potential (E_r) of −28 mV, and E_r shifted by 29.9 mV for a tenfold increase in $[Mg^{2+}]_o$ (Fig. 14*D*), close to the 29 mV/decade change predicted by the Nernst equation for a divalent cation current. More interesting is the fact that the reversal potentials correspond to an $[Mg^{2+}]_i$ of 7.8 mM (±1.9 mM, $n = 27$).

$[Mg^{2+}]_i$ in the wild type was estimated previously to be 0.4 mM (Preston, 1990), but was based on E_r determinations of inward currents at low $[Mg^{2+}]_o$ (0.05–0.5

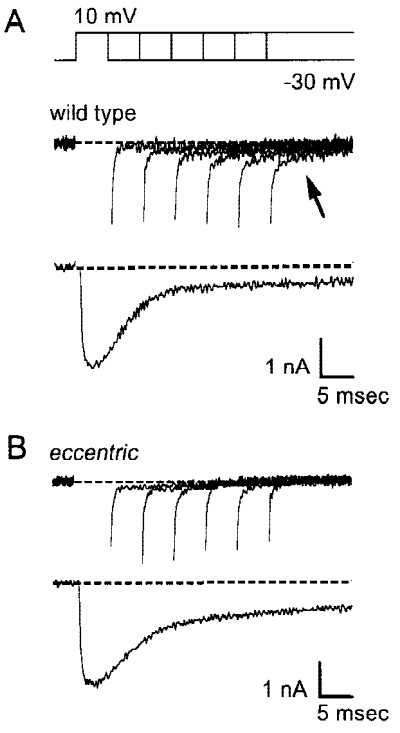

Fig. 6. Rapid development of I_{Mg} upon depolarization. (*A*) Tail currents elicited by depolarizations from −30 to 10 mV that increased in duration from 5 to 30 msec. The inward currents flowing during the voltage step have been blanked to allow the tail currents to be viewed clearly. Note that a slow tail component (τ = 10.7 msec) appeared following a 15-msec step and was prominent at 30 msec (*arrow*). *Lower trace* shows the inward current that was blanked in the traces above. (*B*) The voltage protocol shown in (*A*) above was repeated using an *eccentric* mutant cell bathed in 5 mM Mg^{2+}. Note that the slow inward Mg^{2+} tail seen in the wild type is missing in *eccentric*. The residual tail is associated with deactivation of $I_{Ca(d)}$. *Lower trace* again shows current flowing during the step that has been blanked in the family of traces presented immediately above.

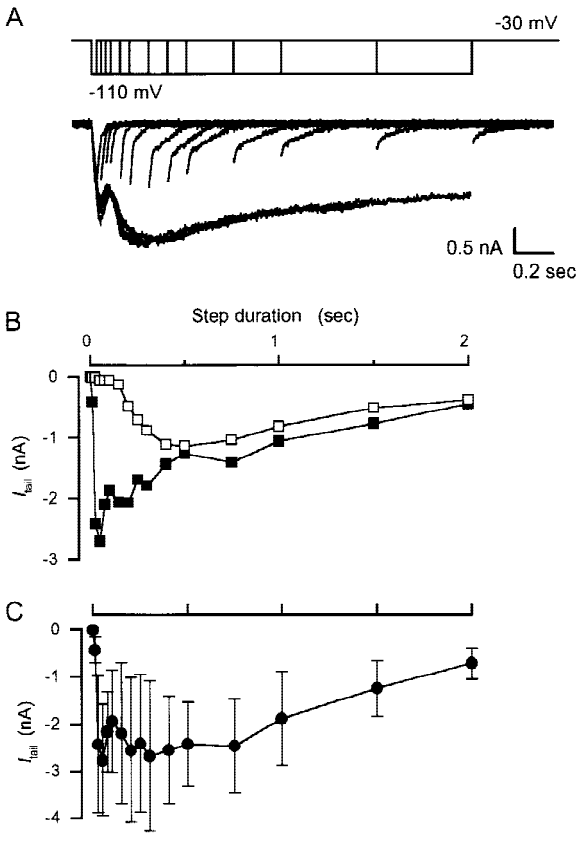

Fig. 7. Development of Mg^{2+} current upon hyperpolarization. (*A*) Currents elicited from wild-type cells in 5 mM Mg^{2+} by steps from −30 to −110 mV of 10 msec to 2-sec duration. (*B*) Amplitudes of the resultant fast-decaying (*filled squares*) and slow-decaying (*open squares*) inward tails plotted as a function of stimulus duration. (*C*) Amplitudes of the combined fast- and slow-tail currents as a function of step duration. Points are means ± SD from 18 cells.

mM) where the slow-decaying tail predominates (Fig. 4). At higher Mg^{2+} concentrations, both fast and slow tails were prominent, so theoretically it should have been possible to measure E_r for both tails over a range of $[Mg^{2+}]_o$. In practice, the current subtraction procedure used in E_r determinations (as described above for *eccentric*) obscured the fine structure of tail currents and made it difficult to determine amplitudes of the individual components with the necessary accuracy. However, it eventually proved possible to estimate fast- and slow-tail reversal potentials in ten wild-type specimens in 5-mM Mg^{2+}. The slow component reversed at 17.9 ± 7.9 mV, corresponding to an $[Mg^{2+}]_i$ of 1.4 mM (±0.5 mM). The fast tail reversed at 6.5 ± 14 mV, corresponding to an $[Mg^{2+}]_i$ of 5.1 ± 5.7 mM.

The analyses above imply that there are at least two Mg^{2+} compartments within *Paramecium*, one at a low concentration (*ca.* 0.4 mM) and one at high concentration (*ca.*

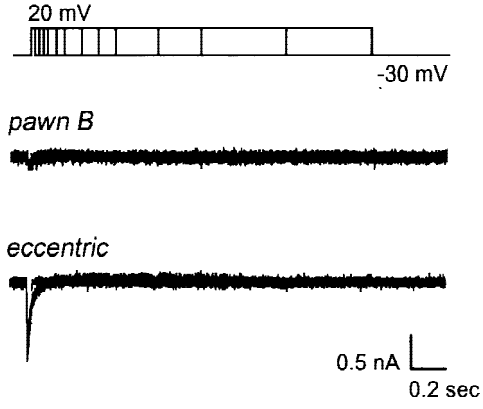

Fig. 8. Suppression of I_{Mg} by mutation. Two mutant strains of *Paramecium* were held at −30 mM in 5 mM Mg^{2+} and then stepped to 20 mV for periods ranging from 25 msec to 2 sec. *Pawn B* mutants lack $I_{Ca(d)}$ and the Ca^{2+}-dependent I_{Mg}, whereas *eccentric* mutant cells specifically lack I_{Mg}. There was no evidence for a Mg^{2+} tail current in either of the current families shown.

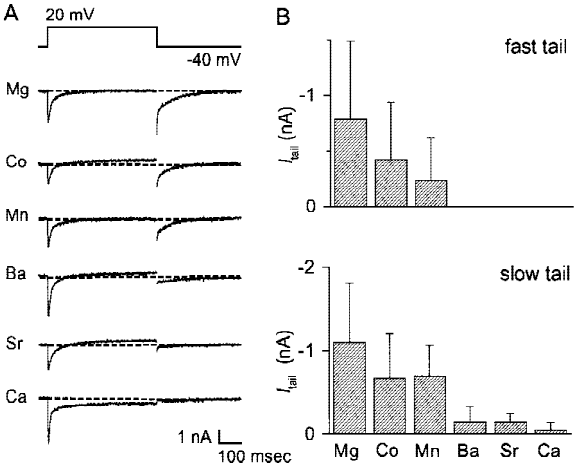

Fig. 9. Ion selectivity of I_{Mg} upon depolarization. (*A*) Cells were held at −40 mV in 1 mM Mg^{2+}, Co^{2+}, Mn^{2+}, Ba^{2+}, Mg^{2+} (+1 mM Ca^{2+}) or 2 mM Ca^{2+} and then stepped to 20 mV for 500 msec to elicit the currents shown. (*B*) Amplitudes of resultant fast-decaying and slow-decaying tail-current components are shown in *upper* and *lower* plots, respectively. Data are mean ± SD determinations from 3 to 7 cells. Note that the value given for Mg^{2+} is cumulative from all cells tested. While the variance appears relatively large, comparison of currents in single cells before and after substituting Mg^{2+} with another ion does reveal statistically significant differences for Ba^{2+}, Sr^{2+}, Ca^{2+} (both tails) and Co^{2+} (slow tail).

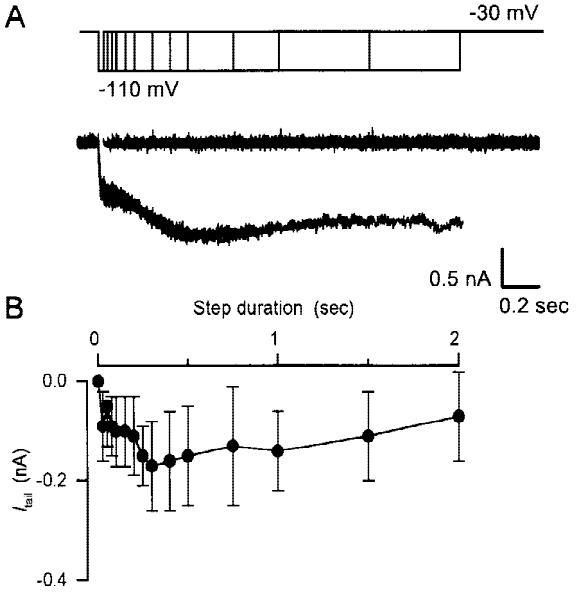

Fig. 10. Currents elicited upon hyperpolarization of *obstinate A* mutants. (*A*) Cells were held under voltage clamp at −30 mV in 5 mM Mg^{2+} and then stepped to −110 mV for periods ranging from 25 msec to 2 sec to elicit the currents shown. (*B*) Amplitudes of the inward tail currents elicited during (*A*) above are plotted as a function of step duration. Points are means ± SD from 7 cells.

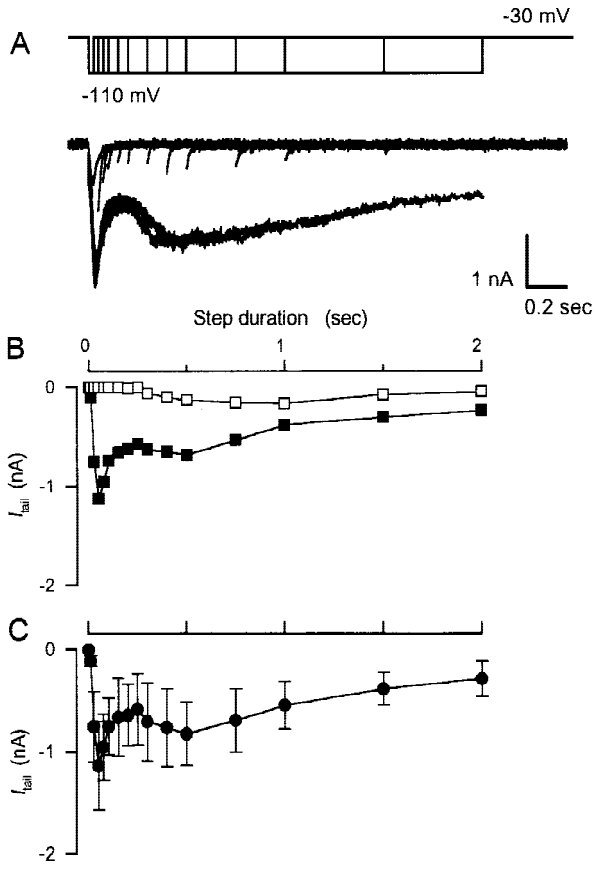

Fig. 11. Mg^{2+} currents elicited upon hyperpolarization of *eccentric*. (*A*) *Eccentric* mutant cells were held at −30 mV in 5 mM Mg^{2+} and then stepped to −110 mV to elicit the currents shown. (*B*) Amplitudes of resulting fast-decaying (*filled squares*) and slow-decaying (*open squares*) tail-current components are plotted as a function of stimulus duration. (*C*) Amplitude of combined tail currents plotted as a function of step duration. Points are means ± SD from 6–11 cells.

8 mM). To determine bulk cytosolic $[Mg^{2+}]_i$, wild-type and *eccentric* mutant cells were loaded with the Mg^{2+}-sensitive fluorescent dye, mag-fura-2. Spectrofluorometric analysis suggested that $[Mg^{2+}]_i$ was 0.38 ± 0.09 mM ($n = 3$) in wild-type cells and 0.32 ± 0.07 mM ($n = 3$) in *eccentric*.

Discussion

The studies described above show that I_{Mg} contributes significantly to membrane excitation and ciliary reversal in *Paramecium* at physiological $[Mg^{2+}]_o$. Close analysis of tails elicited following depolarization and hyperpolarization showed both to decay biphasically, but the depolarization-activated currents appeared to be mediated by a common pathway. The Mg^{2+} current elicited upon hyperpolarization was complex, however, and could be separated into three components. The first, I_{Mg}, could be

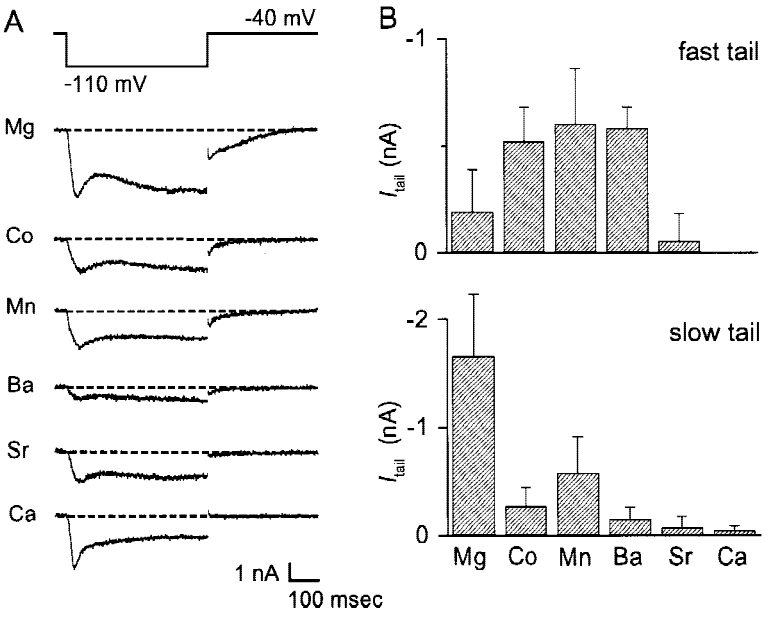

Fig. 12. Ion selectively of the inward tail elicited upon hyperpolarization of the wild type. (*A*) Individual cells were held at −40 mV in 1 mM Mg^{2+}, Co^{2+}, Mn^{2+}, Ba^{2+}, Sr^{2+}, or 2 mM Ca^{2+} and stepped for 500 msec to −110 mV to elicit the currents shown. (*B*) Amplitudes of resulting fast-decaying and slow-decaying tail-current components are provided in *upper* and *lower* plots, respectively. Values represent means ± SD from 5 to 8 cells. The fast tails in Co^{2+}, Mn^{2+}, Ba^{2+} are statistically larger than that in Mg^{2+}, whereas the slow Mg^{2+} tail is statistically larger than any tail following ionic substitution (*see* legend to Fig. 9).

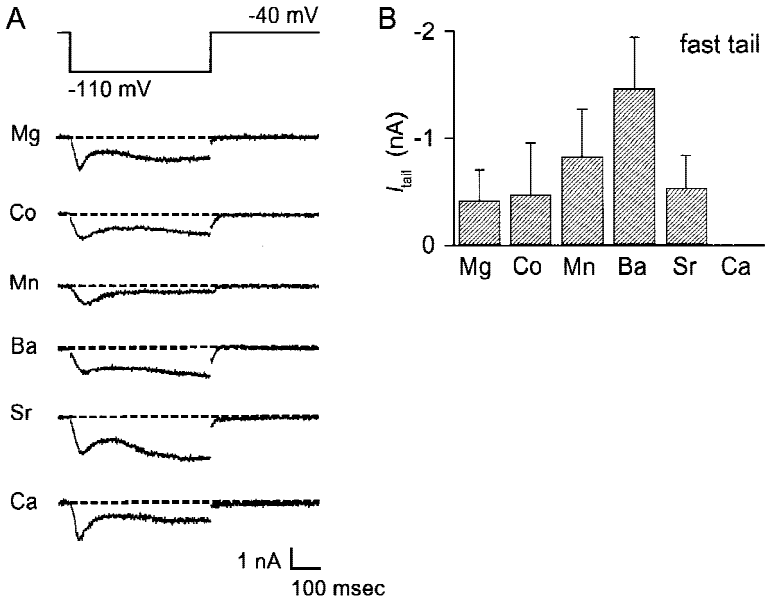

Fig. 13. Ion selectivity of the fast inward tail elicited upon hyperpolarization of *eccentric*. (*A*) Currents elicited by 500-msec steps from −40 to −110 mV from *eccentric* mutant cells bathed in 1 mM concentrations of the ions indicated. (*B*) Amplitudes of resultant fast-decaying inward tails are plotted ± SD, $n = 4$ to 9. The Ba^{2+} value is statistically larger than that for Mg^{2+}.

suppressed by *eccentric* mutation. The second, a nonspecific cation current (I_{NS}), could be suppressed by *obstinate A* mutation and by Ca^{2+}-current inactivation. A third possible component (I_{obs}) appeared as a minor current that was revealed after suppressing I_{Mg} and I_{NS} in *obstinate A.* Reversal potential analysis of the two major Mg^{2+} tails suggested that one reflected bulk cytosolic $[Mg^{2+}]_i$ (0.4 mM) whereas the other reflected fluxes into a high Mg^{2+} compartment (8 mM).

Physiological Role of I_{Mg}

I_{Mg} remains the only example of a current that is strongly Mg^{2+}-specific. Whereas Mg^{2+} currents via nonspecific cation channels have been reported in other cells (Nakatani & Yau, 1988; Narita et al., 1990; Kawa, 1996), the preference of the *Paramecium* conductance for Mg^{2+} over Ca^{2+} (Figs. 9 and 12) is highly unusual, although it may no longer be unique. Pottosin and Schönknecht (1996) recently described a cation channel in spinach thylakoid membranes whose conductance to Mg^{2+} was greater than that to Ca^{2+}, while Beyenbach et al. (1997) presented radiolabel flux data suggestive of a Mg^{2+}-selective pathway in trout renal cells.

Paramecium thrives in freshwater where $[Mg^{2+}]_o$ is low (*ca.* 0.2 and 0.7 mM for soft and hard water, respectively: Machemer & Deitmer, 1985), which had raised questions about whether Mg^{2+} currents elicited and po-

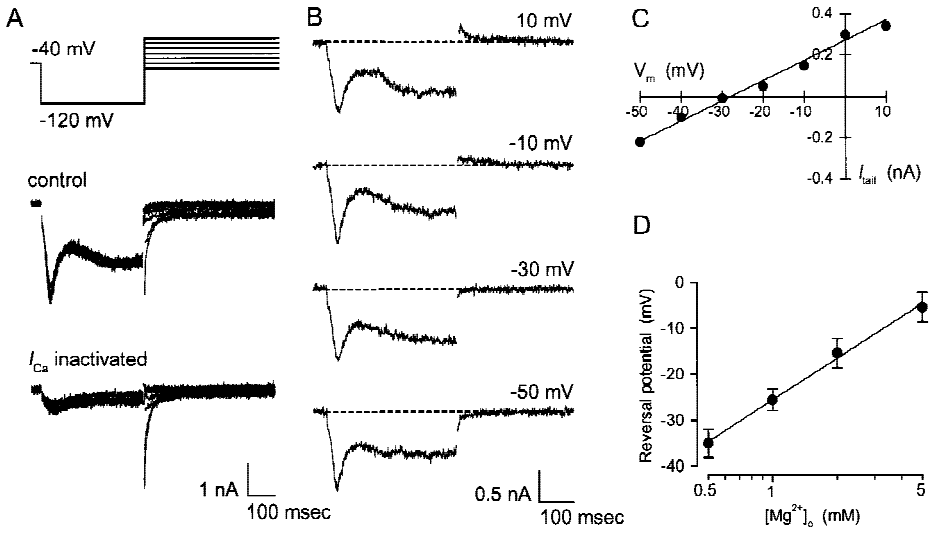

Fig. 14. Reversal analysis of the Mg^{2+} tail current in *eccentric*. (*A*) Upper voltage trace indicates that cells were held at −40 mV in varied $[Mg^{2+}]_o$ and then stepped to −120 mV for 400 msec to elicit current. Tail currents were elicited by stepwise increases in membrane potential from −70 to 30 mV. Current traces show membrane responses to voltage protocol above either before (''control'') or after inactivating $I_{Ca(h)}$ using 4.5-sec steps to −120 mV. (*B*) Four of the difference currents from the traces in (*A*). Membrane potential at which the tail currents were elicited are indicated. (*C*) Amplitudes of the tail currents shown in (*B*) are plotted as a function of the membrane potential at which they were recorded. Note that the tail reverses polarity at −28 mV (E_r). Solid line was fitted by linear regression. (*D*) The procedure described in (*A*) through (*C*) above was repeated using Mg^{2+} concentrations ranging from 0.5 to 5 mM. Reversal potentials have been plotted as a function of $[Mg^{2+}]_o$. Points are means ± SD determinations from 6 to 8 cells. Solid line was fitted by linear regression. E_r changes by 29.9 mV per decade change in $[Mg^{2+}]_o$.

tentiated using forced voltage steps are of physiological significance. $[Mg^{2+}]_i$ in *Paramecium* is also low, however (0.4 mM: *see* Results and Preston, 1990), so even with only 0.2 mM $[Mg^{2+}]_o$, there is still a strong driving force for Mg^{2+} influx provided by the negative V_m. Indeed, if Mg^{2+} were in electrochemical equilibrium across the membrane, $[Mg^{2+}]_i$ should rest at between 5 and 18 mM (for $[Mg^{2+}]_o$ of 0.2 and 0.7 mM, respectively). Several lines of evidence suggest that I_{Mg} is both a physiological and relevant current in *Paramecium*. First, both positive and negative excursions from rest in physiological concentrations of $[Mg^{2+}]_o$ elicited inward currents that were saturable with respect to the magnitude of the activating stimulus (Fig. 2*B*). The ability to specifically inhibit this conductance by single-gene mutation (Preston & Kung, 1994*a*) additionally argues against I_{Mg} being, for example, an artefactual leak current. Second, the duration of backward swimming induced by transferring cells to Mg^{2+} solution correlated well with the $[Mg^{2+}]_o$-dependence of I_{Mg} upon depolarization (Fig. 3*A* and *B*), suggesting that Mg^{2+} entry via this pathway is the cause of the prolonged backward swimming. Again, the ability to specifically block Mg^{2+}-induced backward swimming by mutation (Preston & Kung, 1994*b*) supports the contention that the two events are linked. Third, I_{Mg} activated within 15 msec of step depolarization (Fig. 6*A*). Since an action potential in *Paramecium* can last from tens of milliseconds to seconds, there is a strong likelihood of I_{Mg} contributing significantly to membrane excitability and recovery. Indeed, previous studies have suggested that this current may be involved in modifying the recovery phase of the action potential (Preston & Kung, 1994). Finally, I_{Mg} has been shown recently to couple GTP-receptor binding to repulsion from this nucleotide in *Paramecium* (Clark et al., 1997).

Note that both Mg^{2+}-induced swimming behavior (Fig. 3*A*, *see also* Clark et al., 1997) and the tail current upon depolarization peaked at between 1 and 10 mM $[Mg^{2+}]_o$ and then declined with further increases in concentration. This is consistent with the known Ca^{2+}-dependence of I_{Mg} (Preston, 1990) and the block of $I_{Ca(d)}$ by extracellular Mg^{2+} (Nakaoka et al., 1994).

Mg^{2+} Currents upon Depolarization

Depolarization elicited Mg^{2+} tails that often required two exponents to adequately describe them, but several observations suggested that a single species of membrane conductance mediated both components. Both tails were missing in *pawn B* (Fig. 8), a mutant whose lack of $I_{Ca(d)}$ suggested a common Ca^{2+}-dependence. Both were inhibited fully by *eccentric* mutation (Fig. 8) and both showed a selectivity sequence in which Mg^{2+} was preferred over Ba^{2+} or Ca^{2+} (Fig. 9). The biphasic nature of the tail current's decay could be explained in several ways, but the most plausible is that the two time courses reflect both intrinsic channel closure rates and also the rate at which Ca^{2+} is cleared from the cytosol following excitation.

Evidence for Two Mg^{2+} Conductances upon Hyperpolarization

In contrast, the membrane response to hyperpolarization probably involves two or possibly three distinct pathways. The first (I_{obs}) was relatively small, comprising <0.2 nA of the inward tail elicited following a step to −110 mV in 5 mM Mg^{2+}, and was revealed following inhibition of I_{Mg} and a nonspecific divalent cation current (I_{NS}) by *obstinate A* mutation (Fig. 10). This current was so small that it was difficult to study systematically, but appeared to activate within 25 msec of a step change in potential and to persist for at least 2 sec. This current may correspond to a largely uncharacterized divalent cation conductance suggested by Nakaoka and Iwatsuki (1992) to stimulate increased ciliary beat frequency upon hyperpolarization of *P. caudatum.*

The second component, I_{NS}, was revealed following suppression of I_{Mg} by *eccentric* mutation. This current was characterized by a permeability to Ba^{2+}, Mn^{2+}, Co^{2+}, and Sr^{2+} in addition to Mg^{2+} (Fig. 13*B*) and for its dependence on $I_{Ca(h)}$. The latter could be deduced from the loss of an associated fast-decaying tail when $I_{Ca(h)}$ was inhibited by mutation (Fig. 10) or was inactivated (Fig. 14*A* and Preston, 1990). While the envelope of fast tails shown in Fig. 11*B* (*filled squares*) may be contaminated by $I_{Ca(h)}$ (*see* below), it suggests that I_{NS} activated rapidly during hyperpolarization to −110 mV and was sustained for at least 2 sec. Many *eccentric* mutant cells also exhibited a slow-decaying tail upon hyperpolarization (Fig. 11*B, open squares*). This minor current may have resulted from incomplete suppression of I_{Mg} or, more likely, may have represented current referred to as I_{obs} above. This current was insufficiently large or consistent in *eccentric* to be analyzed thoroughly.

The third Mg^{2+} conductance showed a preference for Mg^{2+} over Ba^{2+} and Ca^{2+} that matched that of the Mg^{2+} current upon depolarization, suggesting that the two are mediated by a common pathway, I_{Mg}. Confirmation of this idea awaits detailed single-channel analysis.

It should be noted that hyperpolarization in Mg^{2+} solution also activates the Ca^{2+} current that allows for activation of I_{Mg} and I_{NS}. On the basis of studies conducted in the absence of Mg^{2+}, $I_{Ca(h)}$ might be expected to contribute an inward peak at 35–80 msec and to be associated with an inward tail current with a time constant of 12.7 msec (Preston et al., 1992). This current might thus have accounted for at least some of the inward transient seen at 50 msec in Fig. 11*B* (*filled squares*) that was attributed to I_{NS}. Millimolar concentrations of Mg^{2+} block $I_{Ca(h)}$, however, and it inactivates fully by 300 msec (Preston et al., 1992). Thus, while this current might have contributed to the tails elicited by steps of short duration in 5 mM Mg^{2+}, it is unlikely that it explained the currents at >300 msec. Support for this belief comes from the fact that I_{NS} was preferentially carried by Ba^{2+}, a cation that inhibits $I_{Ca(h)}$ fully at 1 mM (Preston et al., 1992), and also from reversal potential analysis of I_{NS} in *eccentric* that showed the current to be closely tied to extracellular Mg^{2+} at constant $[Ca^{2+}]$ (Fig. 14).

Compartmentalization of $[Mg^{2+}]_i$ in *Paramecium*

Perhaps the most remarkable and significant finding of these studies is the suggestion that I_{Mg} and I_{NS} reflect fluxes into low- and high-Mg^{2+} compartments, respectively. Spectrofluorometric determinations of $[Mg^{2+}]_i$ in wild-type cells yielded a value of 0.38 mM, which agrees well with values determined from the reversal potential of I_{Mg} (0.39 mM: Preston, 1990) and with equivalent estimates of $[Mg^{2+}]_i$ that are well below electrochemical equilibria in many other cell types (reviewed by Alvarez-Leefmans et al., 1987). *Eccentric* mutant cells contained low $[Mg^{2+}]_i$ also (0.32 mM), yet reversal potential determinations of I_{NS} in *eccentric* yielded a value of 7.8 mM. A limited analysis of the fast tail current in the wild type also placed $[Mg^{2+}]_i$ at high concentrations (*ca.* 6 mM), values that suggest that I_{NS} reflected movement into and out of a compartment that may actually be in electrochemical equilibrium with the cell exterior. These values have to be interpreted with caution because the processing of determining E_r can change $[Mg^{2+}]_i$, but this does not diminish the significance of finding that there are discrete compartments within *Paramecium* in which free Mg^{2+} levels may be regulated independently. This supports earlier suggestions by Grubbs, Collins & Maguire (1984) that Mg^{2+} may be sequestered in two discrete pools in S49 lymphoma cells (based on radiolabel exchange studies). The importance of these findings relates to the idea that Mg^{2+} may be a critical regulator of cell function in eukaryotes. If changes in free Mg^{2+} levels are used by cells to modulate activity, it should be possible to show that Mg^{2+} fluxes and changes in $[Mg^{2+}]_i$ remain contained, much as Ca^{2+} fluxes are spatially segregated to ensure that they do not simultaneously trigger every Ca^{2+}-sensitive process within a cell. *Paramecium*, for example, contains at least two distinct Ca^{2+} conductances. Whereas one is activated upon depolarization and results in ciliary reversal, hyperpolarization-activated Ca^{2+} influx occurs without reversing the cilia, implying that the two fluxes remain functionally and spatially segregated (Preston et al., 1992).

Paramecium remains the only eukaryotic cell in which a clear physiological function for Mg^{2+} fluxes can be demonstrated. It also remains the only eukaryote in which the conductances responsible can be manipulated through genetic mutation. The recent successful application of expression cloning techniques to *Paramecium* (Haynes et al., 1996; Skouri & Cohen, 1997) should soon

also make it possible to describe the various components involved in intracellular free Mg^{2+} homeostasis in *Paramecium* at the molecular level, demonstrating the importance of continued studies of I_{Mg} and the role of $[Mg^{2+}]_i$ in this organism.

I am grateful to J. A. Hammond for technical assistance, to Dr. C. Kung (University of WI-Madison) for kindly providing *Paramecium* mutants, and to Drs. J. Van Houten (University of Vermont), W. E. Crowe and J. M. Russell (Allegheny University of the Health Sciences) for their generosity and help in the use of fluorescent dyes. I would also like to thank the National Institute of General Medical Sciences at the National Institutes of Health for their support (GM51498).

References

Alvarez-Leefmans, F.J., Giraldez, F., Gamiño, S.M. 1987. Intracellular free magnesium in excitable cells: its measurement and its biologic significance. *Can. J. Physiol. Pharmacol.* **65:**915–925

Amalou, Z., Gilbrat, R., Trouslot, P., d'Auzac, J. 1994. Solubilization and reconstitution of the $Mg^{2+}/2H^+$ antiporter of the lutoid tonoplast from *Hevea brasiliensis* latex. *Plant Physiol.* **106:**79–85

Beyenbach, K.W. 1990. Transport of magnesium across biological membranes. *Magnesium Trace Elem.* **9:**233–254

Beyenbach, K.W., Freire, C.A., Kinne-Saffran, E., Kinne, R.K.H. 1997. Transport of magnesium across renal membrane vesicles: evidence for a channel? *Adv. Magnesium Res.* **1:**443–450

Clark, K.D., Hennessey, T.M., Nelson, D.L., Preston, R.R. 1997. Extracellular GTP causes membrane-potential oscillations through the parallel activation of Mg^{2+} and Na^+ currents in *Paramecium tetraurelia. J. Membrane Biol.* **157:**159–167

Cowan, J.A. 1995. The biological chemistry of magnesium. VCH, New York

Dai, L.-J., Quamme, G.A. 1992. Cyclic nucleotides alter intracellular free Mg^{2+} in renal epithelial cells. *Am. J. Physiol.* **262:**F1100–F1104

Flatman, P.W. 1991. Mechanisms of magnesium transport. *Ann. Rev. Physiol.* **53:**259–271

Grubbs, R.D. 1991. Effect of epidermal growth factor on magnesium homeostasis in BC_3H1 myocytes. *Am. J. Physiol.* **260:**C1158–C1164

Grubbs, R.D., Collins, S.D., Maguire, M.E. 1984. Differential compartmentation of magnesium and calcium in murine S49 lymphoma cells. *J. Biol. Chem.* **259:**12184–12192

Grubbs, R.D., Maguire, M.E. 1987. Magnesium as a regulatory cation: criteria and evaluation. *Magnesium* **6:**113–127

Grubbs, R.D., Walter, A. 1994. Determination of cytosolic Mg^{2+} activity and buffering in BC_3H-1 cells with mag-fura-2. *Molec. Cell. Biochem.* **136:**11–22

Grynkiewicz, G., Poenie, M., Tsien, R.Y. 1985. A new generation of Ca^{2+} indicators with greatly improved fluorescence properties. *J. Biol. Chem.* **260:**3440–3450

Günther, T., Ebel, H. 1990. Membrane transport of magnesium. *In:* Metal Ions in Biological Systems. H. Sigel and A. Sigel, editors. pp. 215–225. Marcel Dekker, New York

Günther, T., Vormann, J. 1990. Characterization of Na^+-independent Mg^{2+} efflux from erythrocytes. *FEBS Lett.* **271:**149–151

Gylfe, E. 1990. Insulin secretagogues induce Ca^{2+}-like changes in cytoplasmic Mg^{2+} in pancreatic β-cells. *Biochim. Biophys. Acta* **1055:**82–86

Haynes, J.W., Ling, K.-Y., Saimi, Y., Kung, C. 1996. Toward cloning genes by complementation in *Paramecium. J. Neurogenet.* **11:**81–98

Hinrichsen, R.D., Saimi, Y. 1984. A mutation that alters properties of the calcium channel in *Paramecium tetraurelia. J. Physiol.* **351:**397–410

Hinrichsen, R.D., Schultz, J.E. 1988. *Paramecium:* a model system for the study of excitable cells. *Trends Neurosci.* **11:**27–32

Hwang, D.L., Yen, C.F., Nadler, J.L. 1993. Insulin increases intracellular magnesium transport in human platelets. *J. Clin. Endocrinol. Metab.* **76:**549–553

Ishijima, S., Sonoda, T., Tatibana, M. 1991. Mitogen-induced early increase in cytosolic free Mg^{2+} concentration in single Swiss 3T3 fibroblasts. *Am. J. Physiol.* **261:**C1074–C1080

Kawa, K. 1996. ADP-induced rapid inward currents through Ca2+-permeable cation channels in mouse, rat and guinea-pig megakaryocytes: a patch-clamp study. *J. Physiol.* **495:**339–352

Kung, C. 1971*a*. Genic mutants with altered system of excitation in *Paramecium aurelia.* I. Phenotypes of the behavioral mutants. *Z. Vergl. Physiol.* **71:**142–164

Kung, C. 1971*b*. Genic mutants with altered system of excitation in *Paramecium aurelia.* II. Mutagenesis, screening and genetic analysis of the mutants. *Genetics* **69:**29–45

Lefort-Tran, M., Aufderheide, K., Pouphile, M., Rossignol, M., Beisson, J. 1981. Control of exocytotic processes: cytological and physiological studies of trichocyst mutants in *Paramecium tetraurelia. J. Cell Biol.* **88:**301–311

Machemer, H., Deitmer, J.W. 1985. Mechanoreception in ciliates. *In:* Progress in Sensory Physiology. H. Autrum, D. Ottoson, E.R. Perl, R.F. Schmidt, H. Simazu, W.D. Willis, editors. pp. 81–118. Springer-Verlag, Berlin

Nakaoka, Y., Iwatsuki, K. 1992. Hyperpolarization-activated inward current associated with the frequency increase in ciliary beating of *Paramecium J. Comp. Physiol.* **170:**723–727

Nakaoka, Y., Teunis, P., Weskamp, M., Machemer, H. 1994. Cationic inhibition of Ca current and Ca-dependent ciliary responses in *Paramecium. J. Comp. Physiol.* **174A:**77–82

Nakatani, K., Yau, K.-W. 1988. Calcium and magnesium fluxes across the plasma membrane of the toad rod outer segment. *J. Physiol.* **395:**695–729

Narita, K., Kawasaki, K., Kita, H. 1990. Mn and Mg influxes through Ca channels of motor nerve terminals are prevented by verapamil in frogs. *Brain Res.* **510:**289–295

Oertel, D., Schein, S.J., Kung, C. 1977. Separation of membrane currents using a *Paramecium* mutant. *Nature* **268:**120–124

Oertel, D., Schein, S.J., Kung, C. 1978. A potassium conductance activated by hyperpolarization in *Paramecium. J. Membrane Biol.* **43:**169–185

Okada, K., Ishikawa, S.-E., Saito, T. 1992. Cellular mechanisms of vasopressin and endothelin to mobilize $[Mg^{2+}]_i$ in vascular smooth muscle cells. *Am. J. Physiol.* **263:**C873–C878

Paolisso, G., Sgambato, S., Passariello, N., Giugliano, D., Scheen, A., 'Onofrio, F.D., Lefèbvre, P.J. 1986. Insulin induces opposite changes in plasma and erythrocyte magnesium concentrations in normal man. *Diabetologia* **29:**644–647

Pottosin, L.L., Schönknecht, G. 1996. Ion channel permeable for divalent and monovalent cations in native spinach thylakoid membranes. *J. Membrane Biol.* **152:**223–233

Preston, R.R. 1990. A magnesium current in *Paramecium. Science* **250:**285–288

Preston, R.R., Hammond, J.A. 1997. Phenotypic and genetic analysis of ''*chameleon*,'' a *paramecium* mutant with an enhanced sensitivity to magnesium. *Genetics* **146:**871–880

Preston, R.R., Kung, C. 1994*a*. Inhibition of Mg^{2+} current by single-gene mutation in *Paramecium. J. Membrane Biol.* **137:**203–212

Preston, R.R., Kung, C. 1994*b*. Isolation and characterization of *Paramecium* mutants defective in their response to magnesium. *Genetics* **137:**759–769

Preston, R.R., Saimi, Y. 1990. Calcium ions and the regulation of motility in *Paramecium. In:* Ciliary and Flagellar Membranes. R.A. Bloodgood, editor. pp. 173–200. Plenum Press, New York

Preston, R.R., Saimi, Y., Kung, C. 1990. Evidence for two K^+ currents activated upon hyperpolarization of *Paramecium tetraurelia*. *J. Membrane Biol.* **115:**41–50

Preston, R.R., Saimi, Y., Kung, C. 1992. Calcium current activated upon hyperpolarization of *Paramecium tetraurelia. J. Gen. Physiol.* **100:**233–251

Raju, B., Murphy, E., Levy, L.A., Hall, R.D., London, R.E. 1989. A fluorescent indicator for measuring cytosolic free magnesium. *Am. J. Physiol.* **256:**C540–C548

Richard, E.A., Saimi, Y., Kung, C. 1986. A mutation that increases a novel calcium-activated potassium conductance of *Paramecium tetraurelia. J. Membrane Biol.* **91:**173–181

Romani, A., Scarpa, A. 1992. Regulation of cell magnesium. *Arch. Biochem. Biophys.* **298:**1–12

Saimi, Y., Hinrichsen, R.D., Forte, M., Kung, C. 1983. Mutant analysis shows that the Ca^{2+}-induced K^+ current shuts off one type of excitation in *Paramecium. Proc. Natl. Acad. Sci. USA* **80:**5112–5116

Sébille, S., Millt, J.-M., Maizières, M., Arnaud, M., Delabroise, A.-M., Jacquot, J., Manfait, M. 1996. Spatial and temporal Mg^{2+} signaling in single human tracheal gland cells. *Biochem. Biophys. Res. Commun.* **227:**743–749

Singh, J., Wisdom, D.M. 1995. Second messenger role of magnesium in pancreatic cells of the rat. *Molec. Cell. Biochem.* **149/150:**175–182

Skouri, F., Cohen, J. 1997. Genetic approach to regulated exocytosis using functional complementation in *Paramecium*—identification of the Nd7 gene required for membrane fusion. *Molec. Cell. Biol.* **8:**1063–1071

White, R.E., Hartzell, H.C. 1989. Magnesium ions in cardiac function. Regulator of ion channels and second messengers. *Biochem. Pharmacol.* **38:**859–867